Available online at www.sciencedirect.com
ScienceDirect
Journal of the European Ceramic Society 27 (2007) 3301–3305
www.elsevier.com/locate/jeurceramsoc

Strength enhancement of 2D-SiC$_f$/SiC composites after static fatigue at room temperature

A. Morales-Rodríguez [a,*], M. Moevus [b], P. Reynaud [b], G. Fantozzi [b]

[a] *Departamento de Física de la Materia Condensada, Universidad de Sevilla, Apartado 1065, 41080 Sevilla, Spain*
[b] *Groupe d'Etude de Métallurgie Physique et de Physique des Matériaux (GEMPPM, UMR CNRS 5510), INSA de Lyon, 20 Avenue Albert Einstein, 69621 Villeurbanne, France*

Available online 2 April 2007

Abstract

The fracture behavior of 2D-woven-SiC-fiber/SiC-matrix composites (2D-SiC$_f$/SiC) has been studied under monotonic tensile test conditions in air at room temperature. The specimens statically fatigued at 90% σ_R showed a higher ultimate tensile strength (UTS) and failure strain than those of the original ones. Microstructural observations suggest that the static fatigue process enhances slow crack growth (SCG) mechanisms in fibers and the extensive fiber/matrix debonding after fatigue could be responsible of the enhanced final strength observed. Ultimate tensile stress has been evaluated from mirror radii of broken fibres, although this method turns up to overestimate experimental data. In contrast, the fracture behavior of Nicalon fiber bundles agrees with the results obtained in these composites.

Keywords: Interfaces; Fatigue; Strength; SiC; Nicalon fibers

1. Introduction

Ceramic-matrix composites (CMCs), such as SiC$_f$/SiC, are promising candidates for high-temperature applications as structural materials.[1] The main disadvantages of monolithic ceramics for structural components are their brittleness and low reliability; continuous-fiber-reinforced ceramic-matrix composites are specifically tailored to achieve a highly fracture-resistant material. CMCs combine the chemical stability of monolithic ceramics with appropriate strength and damage tolerance by means of reinforcing fibers that enhance the inherent ceramic brittleness.

It has been stated that the strength of Nicalon-SiC$_f$/SiC composites, tested in air at room temperature, enhances after cyclic fatigue.[2] The origin of this enhancement is not yet well understood, but the authors suggest that it could be related to a decrease of the fiber/matrix shear stress, τ. Low τ values make the composite less sensitive to the nucleation of defects by decreasing both the stress concentrations and the load transfer from matrix to fibers.[2] Similar strength enhancements have been observed in C$_f$/SiC and Hi-Nicalon-SiC$_f$/Si,B,C composites.[3,4]

This work is focused on the influence of the static fatigue during long periods of time (about 120 h) on the residual strength of Nicalon-SiC$_f$/SiC composites and to determine if residual strength of the composites is linked to the previous fatigue damage. Residual tensile tests after static fatigue at different stress levels have been performed. *In situ* fiber strength and shear stress at the fiber/matrix interface have been estimated as a function of loading conditions through the observation of fracture surfaces. Special attention has been also paid to study the matrix damage levels and more particularly the multiple cracking of matrix in longitudinal yarns.

2. Experimental procedure

Specimens of 2D-Nicalon-fiber-reinforced SiC-matrix composites were provided by Snecma Propulsion Solide (France). The composites were fabricated by densifying preforms of 0/90° woven Nicalon NLM 202 fibers (from Nippon Carbon Co., Japan) with SiC deposited by chemical vapor infiltration (CVI). The resulting composites were 15% porous, approximately, with large pores (macropores) located between the plies or at yarn intersections within the plies; much smaller pores are also present within the tows between the different matrix layers. Details of fiber-reinforced SiC composites fabrication are described elsewhere.[5]

* Corresponding author. Tel.: +34 954 556 029; fax: +34 954 612 097.
E-mail address: amr@us.es (A. Morales-Rodríguez).

0955-2219/$ – see front matter © 2007 Elsevier Ltd. All rights reserved.
doi:10.1016/j.jeurceramsoc.2007.02.180

Table 1
List of MTT-deformed specimens indicating the sollicitation conditions, strengths, final strains and Young's moduli

Specimen	Loading rate (N/min)	σ_{UTS} (MPa)	ε_{final} (%)	E_C (MPa)
#1	500	228	0.66	189
#2	100	202	0.48	178
#3	100	225	–	–

The fracture behavior at room temperature in air has been investigated under different uniaxial tensile conditions: monotonic load (MTT, *Monotonic Tensile Test*) and after static fatigue at various stress levels to explore the residual properties (RTT, *Residual Tensile Test*). The mechanical tests have been performed on a servohydraulic machine (INSTRON model 8502) using samples with bone-shape of rectangular section (calibrated length: 8 mm × 3 mm × 40 mm). Samples and test conditions are summarized in Tables 1 and 2.

Fractured specimens were examined using a conventional scanning electronic microscope (SEM, model JEOL JSM-840A) to investigate the characteristic fracture surface morphology of the fibers in order to estimate *in situ* fiber strength. Pull-out lengths have been measured to estimate the shear stress developed during fiber/matrix sliding before the final fracture.[6] Surfaces parallel to the loading axis have been cut using a slow speed saw, polished up to 1 μm diamond paste and chemically etched by the Murakami procedure to exhibit the matrix cracks.

3. Experimental results

Fig. 1 presents σ–ε plots corresponding to the initial monotonic tensile behavior of 2D-SiC_f/SiC composites. The mechanical properties obtained from these tests are collected in Table 1. It is observed that these composites are able to achieve UTS values of 228 MPa and final deformations up to 0.7%. Fig. 2 shows σ–ε plots corresponding to RTT after static loading at two different stress levels of 70% (dashed line) and 90% σ_R (solid line) where the maximal strength measured in MTT has been considered as the reference strength, σ_R, for these composites. The changes observed in σ–ε slopes after static fatigue tests, E_C^D, comparing with the first loading slopes, E_C^F, indicate that damaging processes are developed during static fatigue, decreasing the elastic modulus ($E_C^D < E_C^F$). Young's modulus evolution is negligible up to 60% σ_R static loading conditions (Fig. 2, #5). The mechanical properties obtained from RTTs are collected in Table 2. Note that the strength after static loading at low stress (dashed line) is limited to the monotonic strength found for as-received specimens. In contrast, an enhancement of the residual properties is observed after loading at 90% of rupture stress level; higher strength and larger final deformation have been achieved in "high-stress" post-fatigued composites (solid line). This enhancement of residual properties has not been noted previously after static fatigue.

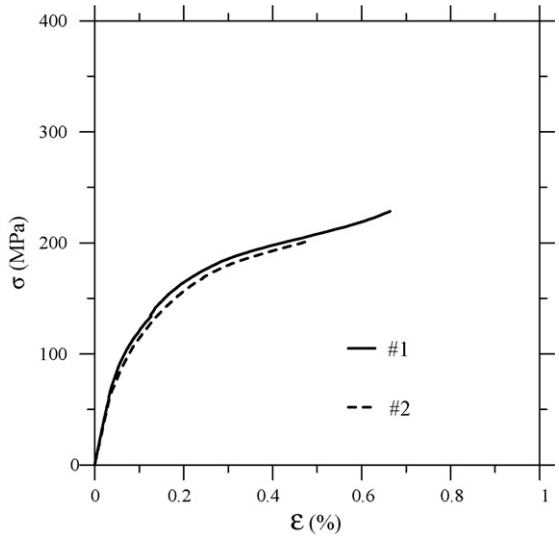

Fig. 1. Monotonic tensile behavior of original specimens loaded at 100 N/min (dashed line) and at 500 N/min (solid line) at room temperature in air.

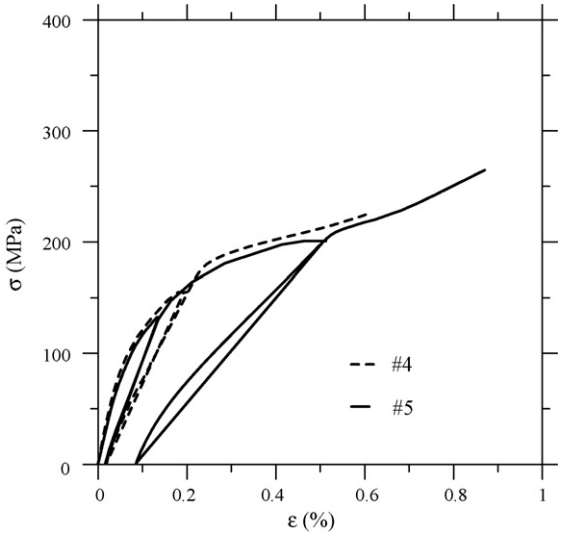

Fig. 2. σ–ε plots from RTT after two different loading conditions in fatigue of 70% (dashed line) and 90% σ_R (solid line) at room temperature in air. These plots show the loading, the static fatigue and the final residual tensile curves.

Table 2
List of RTT-deformed specimens indicating the static fatigue conditions, strengths, final strains and Young's moduli (F: first loading and D: damaged after static fatigue)

Specimen	Fatigue conditions	σ_{UTS} (MPa)	ε_{final} (%)	E_C^F (MPa)	E_C^D (MPa)
#4	100 h, 70% σ_R	225	0.6	197	115
#5	120 h, 90% σ_R	265	0.9	171	82
#6	120 h, 90% σ_R	256	–	–	–

Loading rates of 500 N/min were imposed during monotonic tensile steps.

Microstructural observations have been devoted to characterize the fiber fracture surfaces, pull-out phenomena and matrix cracking to account for the composite mechanical response. The main results obtained are summarized as follows:

(i) The 72% and 82% of fibers in RTT specimens exhibit mirror surfaces after static fatigue at 70% and 90% σ_R, respectively, whereas about the half of fibers in MTT-deformed composites presents mirror surfaces (56%). The previous result suggests that deformation under constant load enhances SCG processes in fibers. The mirror surfaces are well-defined and, in general, the original defect in these Nicalon fibers is associated to the fiber surface, but is too small to be observed (Fig. 3). Measurements of mirror surfaces radii indicate that similar critical crack sizes are observed in both testing conditions.

(ii) The pull-out length is shorter after static fatigue, $l_{RTT} = (34 \pm 2)\,\mu m$, than for original specimens, $l_{MTT} = (58 \pm 4)\,\mu m$. Interfacial debonding between fibers and matrix has been systematically observed for pulled-out fibers. Fig. 4 shows a typical micrograph of pulled-out fibers from a RTT-deformed composite.

(iii) The distribution of the intercracking distance of the SiC matrix has been studied to compare multicracking damage of composites. Fig. 5 shows that the mean matrix-intercracking distances decreases with increasing final stress levels acting on the specimens. Data from two additional tests performed to compare the influence of monotonic and static loading on the matrix damage are also included in Fig. 5 (specimens were loaded below to final fracture stress values until 80% σ_R in case of MTT (#7) and 70% σ_R during 90 h for the static fatigue test (#8) and then, the intercracking distribution was studied for these non-fractured specimens). No differences with global behavior have been deduced from these experiences meaning that both loading conditions induce similar matrix damage characteristics where the key role is played by the final stress level carried.

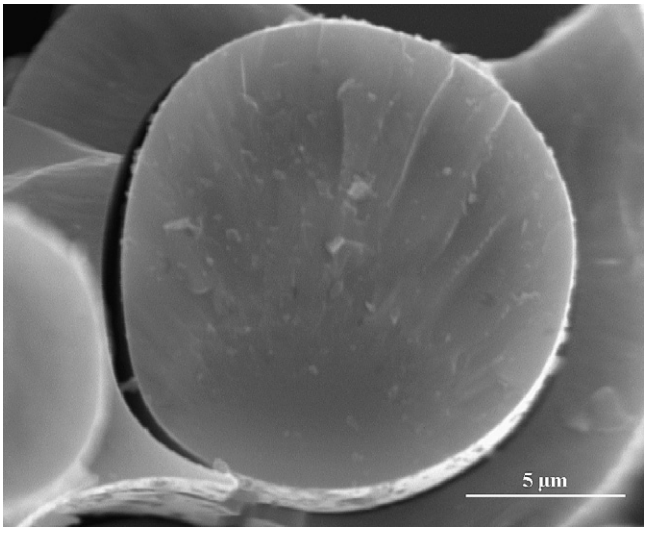

Fig. 3. Distinct mirror surface developed in 2D-SiC_f/SiC composites where it is not possible to identify the initial defect. Note the interfacial debonding between fiber and matrix.

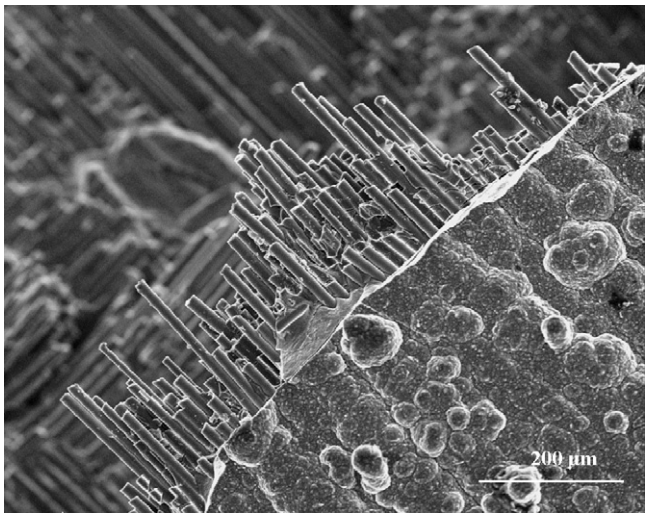

Fig. 4. Pulled-out fibers emerging from the fracture plane in specimen #4.

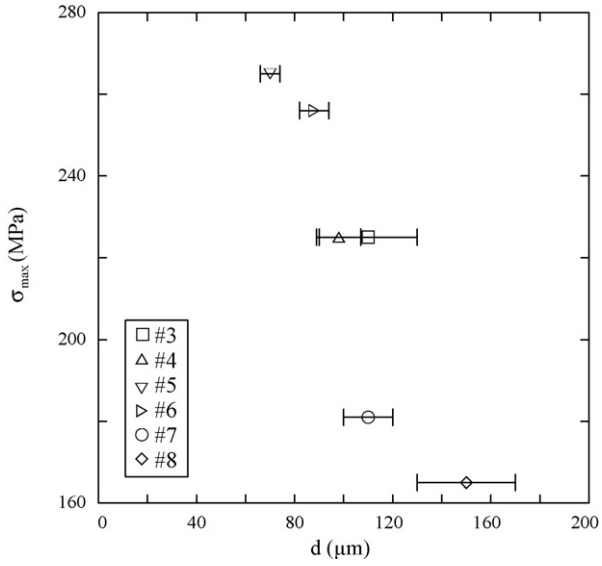

Fig. 5. Matrix-intercracking distance (d) vs. final stress level plot showing a correlation between maximum final stress applied and matrix damage: the higher stress, the shorter intercracking distance.

4. Discussion

4.1. *In situ* fiber strength and fiber/matrix interfacial shear stress of 2D-SiC_f/SiC composites

In situ fiber strength in the composites was evaluated from the measured mirror radii using the following empirical relationship[7]:

$$\sigma_f r_m^{1/2} = A_m, \quad (1)$$

where r_m is the mirror radius, σ_f the *in situ* fiber tensile strength and A_m is the mirror constant. The value of $A_m = 3.5\ \text{MPa m}^{-1/2}$ has been considered in this study following the work of Thouless

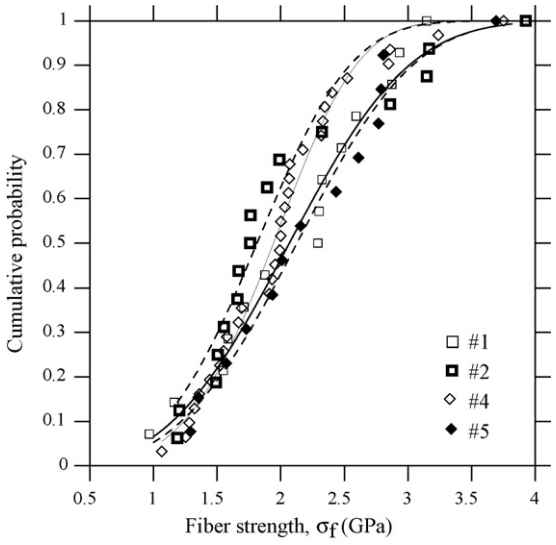

Fig. 6. Statistical distributions of *in situ* fiber tensile strength.

et al.[8] By plotting the cumulative distribution of σ_f (Fig. 6) measured on many fibers (more than 20 fibers/specimen), the shape factor, m, and the scale parameter of the fibers, σ_0, has been ascertained from the Weibull function given by Eq. (2):

$$P(\sigma_f) = 1 - \exp\left[-\left(\frac{\sigma_f}{\sigma_0}\right)^m\right]. \quad (2)$$

These statistical parameters have been used to predict the ultimate strength of composites following Eq. (3) proposed by Curtin[6]:

$$\sigma_{UTS}^{mirror} = V_f \sigma_0 \left(\frac{2}{m+2}\right)^{1/m+1} \left(\frac{m+1}{m+2}\right), \quad (3)$$

where V_f is the volume fraction of fibers in the loading direction (in this study $V_f = 0.2$). A comparison between predicted and measured values of σ_{UTS} is presented in Table 3. Even if a significant fraction of the fibers exhibit well-defined mirror surfaces, it seems that the fracture mirror approach overestimates the UTS values experimentally obtained.

The *in situ* scale parameter, σ_0, has been also used to calculate the fiber/matrix shear stress, τ, using the pull-out length measured on fractured specimens by means of the following expression[6]:

$$\tau = \frac{\lambda(m) r \sigma_0}{4l}, \quad (4)$$

where λ is a m-dependent prefactor that has been taken for a value equal to 1 based on[6] and r is the mean radius of the fiber ($r = 7.25$ μm for NLM 202 Nicalon fibers).

The difference in fiber pull-out lengths measured results in apparent interfacial shear stress values of 80 and 120 MPa for MTT- and RTT-specimens, respectively. There is no physical explanation of such increase of interfacial shear stress due to static fatigue. On the other hand during RTT an additional matrix multicracking can be introduced leading to a saturation of the matrix cracking; in that case, the pull-out length is not representative of the actual value of the interfacial shear stress. Complementary tests are now in progress, using the microindentation technique, to confirm this hypothesis.

4.2. A fiber tows-based approach to explain the 2D-SiC$_f$/SiC composites tensile strength

Although the *in situ* properties of fibers and fiber/matrix interfaces in the composite material is commonly used to infer the macroscopic mechanical properties of CMCs as the tensile strength, UTS, from the strength of the fibers and the shear stress developed during fiber/matrix sliding before the final fracture,[6] the previous analysis of our results is not sufficient to describe the UTS experimentally obtained.

Regarding Figs. 1 and 2, the final linearity of σ–ε curves (except for #2 case) and the large final strains achieved suggest that fiber tows could be the entity responsible for the ultimate failure in these composites, better than individual fiber characteristics.[9] The extensive fiber/matrix debonding stated at microstructural observations supports the previous hypothesis. Debonding phenomena could be strongly determined by matrix-intercracking distances after static loading: the shorter intercracking level, the stronger debonding. Then, the final unloading-reloading performed on fatigued-specimens favours *full* fiber/matrix debonding in *high-stress* fatigued-specimens, achieving larger deformations. Under lower loading conditions it is expected to achieve higher matrix-intercracking distances making more difficult the full fiber/matrix debonding and, therefore, hindering the tow's or individual fiber's elongation. The previous argument justifies the improvement in final strength obtained after static fatigue at 90% respect to 70% σ_R case.

Recently, Calard and Lamon[10] have presented a model for the σ_{UTS} of composites considering the force–strain curves for Nicalon NLM 202 fiber bundles. The final tensile strength of composites, σ_{UTS}^{tows}, is approximately given by the following

Table 3
Comparison between ultimate strengths predictions obtained from *in situ* fiber strength,[6] single fibers and fiber tows[10] approaches

Specimen	σ_{UTS}^{exp} (MPa)	m	σ_0 (GPa)	σ_{UTS}^{mirror} (MPa)	σ_{UTS}^{tows} (MPa)	σ_{UTS}^{fiber} (MPa)
#1	228	3.2	2.3	298	265	238
#2	202	3.6	2.0	262	192	172
#4	225	4.2	2.1	286	221	216
#5	265	3.4	2.4	312	292	324

The statistical parameters obtained from data plotted in Fig. 6 are included.

equations[10]:

$$\sigma_{\mathrm{UTS}}^{\mathrm{tows}} = V_{\mathrm{f}}\sigma_{\mathrm{tow}}, \quad (5)$$

$$\sigma_{\mathrm{tow}} = \frac{F}{N_{\mathrm{t}}(1-\alpha_{\mathrm{C}})\pi r^2}, \quad (6)$$

where V_{f} is the volume fraction of longitudinal fiber tows in the composites, σ_{tow} the tow strength, F the force operating on the tow, N_{t} the nominal number of fibers/tow, α_{C} the critical value of the ratio of the number of broken fibers N to the total number of fibers N_{t} (when the surviving fibers are unable to carry the applied load) and r is the mean fiber radius.

Table 3 presents the values of ultimate strength calculated from previous equations. The critical fraction of broken fibers has been calculated considering that the neighbour overloading of fibers interact (global load sharing).[11] The ultimate strength has also been calculated from single SiC-fibers data ($E = 180$ GPa[10]), $\sigma_{\mathrm{UTS}}^{\mathrm{fiber}}$, considering the final deformations achieved by the composites. Results from predictions collected in Table 3 show that both tows and single fibers are accurate to predict the final composite strength tendency experimentally obtained, better than considering the mirror approach (see Section 4.1).

5. Conclusions

This work points out that the extensive fiber/matrix debonding could be related to the strength enhancement observed in statically fatigued 2D-SiC$_{\mathrm{f}}$/SiC composites. The σ–ε curves indicate that multicracking of the matrix is saturated near the fracture of the composite. Hence, UTS of these composites is well described by fracture behavior of bundles and statistical distribution of individual fiber failures. However, analysis based on the mirror zone of the fibers' fracture surface is less accurate.

Acknowledgements

The authors would like to thank Snecma Propulsion Solide (France) and the programs of *Ayudas de Perfeccionamiento de Doctores de la Junta de Andalucía* and *Ayudas de Movilidad de Ayudantes de la Universidad de Sevilla* (Spain) for supporting this research. We are grateful to Dr. M. R'Mili for his helpful discussion.

References

1. Naslain, R., Design, preparation and properties of non-oxide CMCs for application in engines and nuclear reactors: an overview. *Comp. Sci. Technol.*, 2004, **64**, 155–170.
2. Mizuno, M., Zhu, S., Nagano, Y., Sakaida, Y., Kagawa, Y. and Watanabe, M., Cyclic-fatigue behavior of SiC/SiC composites at room and high temperatures. *J. Am. Ceram. Soc.*, 1996, **79**, 3065–3077.
3. Shuler, S. F., Holmes, J. W. and Wu, X., Influence of loading frequency on the room-temperature fatigue of carbon-fiber/SiC-matrix composites. *J. Am. Ceram. Soc.*, 1993, **76**, 2327–2336.
4. Penas, O., Etude de composites SiC/SiBC à matrice multiséquencée en fatigue cyclique à hautes températures sous air. PhD Thesis. INSA Lyon, Villeurbanne, France, 2002.
5. Stinton, D. P., Caputo, A. J. and Lowden, R. A., Synthesis of fiber-reinforced SiC composites by chemical vapor infiltration. *Am. Ceram. Soc. Bull.*, 1986, **65**, 347–350.
6. Curtin, W. A., Theory of mechanical properties of ceramic-matrix composites. *J. Am. Ceram. Soc.*, 1991, **74**, 2837–2845.
7. Melchosky, J. J., Freiman, S. W. and Rice, R. W., Fracture surface analysis of ceramics. *J. Mater. Sci.*, 1976, **11**, 1310–1319.
8. Thouless, M. D., Sbazeiro, O., Sigl, L. S. and Evans, A. G., Effect of interface mechanical properties on pullout in SiC-fiber-reinforced ceramic matrix composites. *J. Am. Ceram. Soc.*, 1989, **72**, 525–532.
9. Lamon, J. A., A micromechanics-based approach to the mechanical behavior of brittle-matrix composites. *Comp. Sci. Technol.*, 2001, **61**, 2259–2272.
10. Calard, V. and Lamon, J., Failure of fiber bundles. *Comp. Sci. Technol.*, 2004, **64**, 701–710.
11. Fantozzi, G., Reynaud, P. and Rouby, D., Thermomechanical behaviour of long fibres ceramic-ceramic composites. *Sil. Ind.*, 2002, **66**, 109–119.